The role of diffusion induced electro-osmosis in the coupling between hydraulic and ionic fluxes through semipermeable clay soils

(Article begins on next page)

29 November 2022

Technical Paper

The role of diffusion induced electro-osmosis in the coupling between hydraulic and ionic fluxes through semipermeable clay soils

Nicolò Guarena [*], Andrea Dominijanni, Mario Manassero

Department of Structural, Geotechnical and Building Engineering, Politecnico di Torino, Corso Duca degli Abruzzi 24, 10129 Torino, Italy

Abstract

Most of the experimental research conducted to date has provided evidence on the semipermeable membrane behaviour of smectite-rich clay soils, the extent of which is typically quantified through the reflection coefficient, when the permeant (electrolyte) solution contains a single monovalent or divalent salt. Under such conditions, the osmotic flow of solution is controlled to a great extent by the different accessibility of ions and water molecules to the soil porosity, which is referred to as the chemico-osmotic effect. However, theoretical simulations of coupled solute and solvent transport suggest that, when two or more cations that diffuse in water at different rates are present simultaneously in the permeant solution, the electro-osmotic effect, which stems from the condition of null electric current density through the porous medium, can be enhanced compared to the case of a single salt to such an extent that it becomes comparable to or even greater than the chemico-osmotic effect. An original closed-form analytical solution to the problem of calculating the diffusion potential, which in turn controls the magnitude of the electro-osmotic effect, is here illustrated, and the relative importance of the aforementioned contributions to multi-electrolyte systems is examined through the interpretation of laboratory test results from the literature pertaining to a bentonite amended clay soil in equilibrium with aqueous mixtures of potassium chloride (KCl) and hydrochloric acid (HCl). The proposed mechanistic model is shown to be able to quantitatively capture the impact of both chemico-osmosis and electro-osmosis on the measured reflection coefficient of smectite clays, thereby breaking new ground in the experimental and theoretical research on the osmotic properties of engineered clay barriers in contact with mixed aqueous electrolyte solutions.
© 2022 Production and hosting by Elsevier B.V. on behalf of The Japanese Geotechnical Society. This is an open access article under the CC BY-NC-ND license (http://creativecommons.org/licenses/by-nc-nd/4.0/).

Keywords: Chemico-osmosis; Diffusion potential; Electro-osmosis; Landfill liners; Reflection coefficient; Smectite clays

1. Introduction

Coupled flow phenomena are relevant for a number of geoenvironmental applications that involve the use of engineered clay barriers (e.g., geosynthetic clay liners and soil-bentonite mixtures) for the containment of polluted fluids in the subsoil, and the mechanisms that underlie such phenomena have therefore been the subject of both experimental and theoretical research (Manassero and Dominijanni 2003; Mitchell and Soga 2005; Dominijanni et al. 2013; Medved and Černý 2013; Shackelford 2013; Shackelford et al. 2019). The coupling between hydraulic, ionic and electrical fluxes and non-conjugated driving forces through smectite-rich clay soils, which represent the primary components of the aforementioned barriers, results from the semipermeable membrane behaviour, i.e., the ability to partially restrict the migration of anions through pores that are freely accessible to water (H_2O) molecules as a consequence of the electrical interactions that occur between the ions in the pore solution and the negatively charged smectite minerals. Among coupled flow phenomena, the term "osmosis" is used to refer broadly to the movement

---

of the water that is induced by gradients in the intensive properties of the bulk solution other than the hydraulic head (Kemper and Rollins 1966; Groenevelt and Bolt 1969; Mitchell et al. 1973; Fritz 1986; Mitchell 1991; Yeung and Mitchell 1993; Dominijanni and Manassero 2005, 2012a; Malusis et al. 2012; Musso et al. 2017; Guarena et al. 2020).

In the absence of an externally applied electric potential difference, the non-hydraulic component of water movement in porous media, as driven by a gradient in the ionic concentrations, is commonly referred to as "chemical osmosis," which suggests that the unbalance in osmotic pressure that occurs between the pore and external bulk solutions is the only cause of the coupled phenomenon. Accordingly, the extent to which clay soils exhibit membrane behaviour is quantified through the laboratory measurement of the so-called "chemico-osmotic efficiency coefficient," represented by ω, which is expected to range from zero, for non-semipermeable porous media, to unity for ideal or perfect semipermeable porous media that prevent all the anions from entering the pores (Malusis and Shackelford 2002a, 2002b; Yeo et al. 2005; Henning et al. 2006; Evans et al. 2008; Kang and Shackelford 2010, 2011; Mazzieri et al. 2010; Bohnhoff and Shackelford 2013, 2015; Di Emidio et al. 2015; Malusis et al. 2015, 2020; Malusis and Daniyarov 2016; Shackelford et al. 2016; Meier and Shackelford 2017; Sample-Lord and Shackelford 2018; Fu et al. 2021a, 2021b).

In terms of uncharged porous media, the aforementioned rationale provides a comprehensive understanding of the microscale mechanisms that govern osmotically induced water movement, since the selective restriction of the solutes can only be attributed to steric hindrance, which arises when the molecules are larger in size than the membrane pores. However, this interpretation does not explain several particular features that are observed in flow behaviour when an electrically charged porous medium is interposed between electrolyte solutions of different concentrations (Fujita and Kobatake 1968; Woermann 1968; Sasidhar and Ruckenstein 1982; Hijnen and Smit 1995). One of the most notable phenomena, which requires considering additional mechanisms beyond chemico-osmosis to obtain an exhaustive interpretation of the experimental evidence, is the occurrence of the so-called "negative anomalous osmosis," $\omega < 0$, whereby the liquid flux takes place from the more concentrated solution side to the dilute solution side under isobaric conditions. Negative anomalous osmosis has repeatedly been observed in laboratory experiments conducted with both synthetic membranes (Abrams and Sollner 1943; Tasaka et al. 1969; Röttger and Woermann 1993) and with clay soils (Kemper and Quirk 1972; Elrick et al. 1976; Olsen et al. 1989; Keijzer et al. 1999) in equilibrium with aqueous solutions of a single electrolyte.

Under isothermal conditions, any divergence in the osmotic behaviour of fine-grained soils, i.e., with respect to that expected for pure chemico-osmosis, should be related to the build-up of an electro-osmotic effect. As documented in the geotechnical engineering literature (Eykholt and Daniel 1994; Mitchell and Soga 2005), because of the presence of non-equivalent concentrations of cations and anions within the pore solution, the generation of an electric potential difference across a clay layer leads to a net transfer of momentum to the water molecules and to a resulting liquid flux in the cation migration direction, i.e., from the anode to the cathode. In the absence of an externally applied electric field between the clay boundaries, the electric potential difference at null volumetric liquid flux, which is also referred to as the "diffusion potential," spontaneously develops in response to the different diffusivities and electrochemical valences of the ionic species, and its magnitude is such that the condition of a null electric current density is satisfied (Helfferich 1962; Lakshminarayanaiah 1965; Groenevelt and Bolt 1969; Kemper et al. 1972; Appelo and Wersin 2007). Accordingly, the measured ω parameter that results from membrane testing under closed-system conditions (Shackelford 2013) includes both a chemico-osmotic component and a diffusion induced electro-osmotic one, and the term "reflection coefficient" may therefore be regarded as being more appropriate when referring to the aforementioned phenomenological parameter.

Provided the passage of electrons between the specimen boundaries is hindered (i.e., non-short-circuited conditions), the available experimental evidence on the semipermeable membrane behaviour of smectite clays shows a relatively limited, if not negligible, contribution of diffusion induced electro-osmosis, compared to chemico-osmosis, and the former mechanism has therefore only received limited attention by geoenvironmental researchers. However, most membrane tests that have been conducted were carried out on clay specimens in equilibrium with single-salt solutions and, thus, they did not account for the influence of the simultaneous presence of three or more different ions in the pore solution. In view of the relevance of the latter conditions for the assessment of the field performance of engineered clay barriers, the objective of this paper is to present a theoretical framework that allows the osmotic phenomena in clay soils to be modelled in both three-ionic systems, for which an exact analytical solution is derived to calculate the diffusion potential, and in systems containing an unspecified number of ionic species, which can be investigated through approximate analytical solutions as already discussed, albeit in a preliminary fashion, by Guarena et al. (2021a). The ability of the proposed theoretical framework to capture the effect of the different mobilities of the cation species contained in the pore solution is verified through an interpretation of the results of the laboratory tests conducted by Tang et al. (2014, 2015).

2. Theoretical framework

Most mechanistic models that have been developed for the simulation of transport phenomena through fine-

porous charged membranes rely on the Navier-Stokes equation to determine the volumetric liquid flux, q, on the Nernst-Planck equation to determine the molar flux of the i-th ionic species, J_i, and on the Poisson-Boltzmann equation to determine the distribution of the electrostatic potential over the pore cross-section. Two different approaches may be pursued to find a solution to the nonlinear differential system of equations.

According to the first approach, which has come to be known as the "space-charge model," the aforementioned set of equations is solved numerically for a specified geometry of the conductive capillaries, without any additional simplifying assumption (Gross and Osterle 1968; Sasidhar and Ruckenstein 1982; Hijnen and Smit 1995), or analytically under further hypotheses about the concentration distributions of the cations and anions in the diffuse double layers (DDLs) and the ratio of the DDL thickness to the pore size (Jacazio et al. 1972; Groenevelt and Elrick 1976; Hijnen et al. 1985; Smit 1989; Yaroshchuk 2011). Albeit potentially applicable to a large variety of scenarios, the high computational effort that is required for the numerical integration of the space-charge model generally restricts its use to membranes that separate aqueous solutions of a single electrolyte, and the investigation of unusual phenomena that arise in electrolyte mixtures is therefore difficult to access whenever the actual pore-scale distribution of the electric potential is simulated.

The second approach, which has come to be known as the "uniform-potential model," dates back to the works of Schmid (1950) and Schlögl (1955), and it assumes that the electric potential does not vary over the pore cross-section, neglecting the dispersive effects that are caused by the microscale fluctuations of the state variables and the velocity field. Although the assumption of a uniform potential profile leads to some errors for high ionic concentrations, this does not seriously limit the applicability of such an approach which, unlike the previous one, allows fluxes and transport coefficients to be calculated for multi-ionic systems with relatively little computational effort (Cwirko and Carbonell 1989). In addition to its versatility, the uniform-potential model does not require any specification of the microstructure of the porous medium, provided that it can be considered homogeneous at the representative elementary volume scale, and hence this approach results to be particularly suitable to investigate the semipermeable properties of membranes with complex and hierarchical pore structures, such as smectite clays (Leroy et al. 2006; Revil and Linde 2006; Jougnot et al. 2009; Dominijanni et al. 2013, 2018; Manassero et al. 2018; Manassero 2020; Guarena et al. 2021b; Malusis et al. 2021).

Under the hypothesis of dilution of the ions dissolved in the pore solution, the coupling between individual ionic fluxes can be neglected other than by electromigration and advection, and the uniform-potential model therefore yields the following expressions for the macroscopic (i.e., upscaled through a volume-averaging technique) Navier-Stokes and Nernst-Planck equations of fully saturated semipermeable porous media (Dominijanni et al. 2006; Dominijanni and Manassero 2012b):

$$q = -k_\varphi \left(\frac{\mathrm{d}\bar{h}}{\mathrm{d}x} + \frac{F}{\gamma_w} \sum_{i=1}^{N} z_i \bar{c}_i \frac{\mathrm{d}\bar{\varphi}}{\mathrm{d}x} \right) \tag{1a}$$

$$J_i = q\bar{c}_i - nD_i^* \frac{\mathrm{d}\bar{c}_i}{\mathrm{d}x} - nz_i \frac{F}{RT} D_i^* \bar{c}_i \frac{\mathrm{d}\bar{\varphi}}{\mathrm{d}x} \quad \text{for } i = 1, \ldots, N \tag{1b}$$

where k_φ is the hydraulic conductivity at zero electric potential gradient, $\bar{h}$ is the hydraulic head in the pore solution, x is the coordinate along the macroscopic transport direction, γ_w is the water unit weight (9.81 kN/m³), F is Faraday's constant (9.6485×10^4 C/mol), N is the total number of ionic species ($N \geq 2$), z_i is the electrochemical valence of the i-th ionic species, $\bar{c}_i$ is the molar concentration of the i-th ionic species in the pore solution, $\bar{\varphi}$ is the electric potential in the pore solution, n is the soil porosity, $D_i^* = \tau_m D_{0,i}$ is the effective diffusion coefficient of the i-th ionic species, τ_m is the matrix tortuosity factor, which accounts for the geometry of the pore network accessible to diffusion, $D_{0,i}$ is the free-solution or aqueous-phase diffusion coefficient of the i-th ionic species, R is the universal gas constant (8.314 J/mol·K) and T is the absolute temperature.

The electric potential in the pore solution differs from the electric potential in the external bulk solution, φ, which is hypothesised to be in thermodynamic equilibrium with the porous medium at its boundaries. The difference between $\bar{\varphi}$ and φ is known as the phase-boundary or Donnan potential, $\bar{\psi}$, and it can be related to the ratio of the concentration of the i-th ionic species in the pore solution to that in the external bulk solution, c_i, which is also referred to as the ionic partition coefficient, Γ_i, by imposing the condition of equality between the corresponding electrochemical potentials at the macroscopic scale:

$$\Gamma_i = \frac{\bar{c}_i}{c_i} = \exp\left(-z_i \frac{F}{RT} \bar{\psi} \right) \tag{2}$$

The Donnan potential can be determined by substituting Eq. (2) in the following statement of overall electroneutrality in the membrane phase:

$$\bar{c}_{sk} = \sum_{i=1}^{N} z_i \bar{c}_i \tag{3}$$

where $\bar{c}_{sk}$ is the fixed charge concentration referred to the pore volume, which depends on both the surface charge density carried by the solid skeleton and on the soil fabric (Dominijanni et al. 2018, 2019a).

The condition of equality between the chemical potentials of the water in the pore and bulk solutions at the macroscopic scale allows the hydraulic head in the pore solution to be determined as follows:

$$\bar{h} = h + \frac{\bar{\Pi} - \Pi}{\gamma_w} \tag{4}$$

where h is the hydraulic head in the external bulk solution, $\bar{\Pi} = RT\sum_{i=1}^{N}\bar{c}_i$ is the osmotic pressure in the pore solution and $\Pi = RT\sum_{i=1}^{N}c_i$ is the osmotic pressure in the external bulk solution.

As evidenced above, the osmotic pressure is here calculated through the van't Hoff (1887) expression, consistently with the hypothesis of ideal (i.e., infinitely dilute) solutions. Such a calculation approach has been observed to cause an error of the estimated osmotic pressure that is no greater than 7% for lower salt concentrations than 100 mM, compared to the more general expression based on the assessment of the water (H_2O) activity of the salt solutions (Fritz et al. 2020).

An additional relationship is required in the absence of an external electric field to solve the transport equation set under non-short-circuited conditions. Indeed, the ionic fluxes are necessarily such that their sum, expressed in terms of charge equivalents and corresponding to the electric current density, I, is equal to zero in order to prevent a net transfer of the electric charge through the porous medium and, hence, to preserve the electroneutrality condition:

$$I = F\sum_{i=1}^{N} z_i J_i = 0 \tag{5}$$

2.1. Physical interpretation of the reflection coefficient of clays

A physical interpretation of the reflection coefficient of clays in aqueous solutions of two or more electrolytes can be obtained by resorting to the outlined mechanistic model, which has been formulated using the real state variables in the membrane phase (i.e., $\bar{h}$, $\bar{c}_i$ and $\bar{\varphi}$) instead of the virtual state variables in the bulk phase (i.e., h, c_i and φ). If the aforementioned phenomenological parameter is determined via a testing apparatus that allows the hydraulic head difference, or conjugated force, to be measured across the clay specimen for an applied osmotic pressure difference, or non-conjugated force, while the volumetric liquid flux (direct flux) is hindered, the global value of the reflection coefficient at steady state, ω_g, is given by (Van Impe et al. 2003; Malusis et al. 2012):

$$\omega_g = \left[\frac{\gamma_w(\Delta h)_{ss}}{\Delta\Pi}\right]_{q=0;I=0} \tag{6}$$

where $(\Delta h)_{ss}$ and $\Delta\Pi$ are the differences in the steady-state hydraulic head and in the osmotic pressure of the bulk solution across the porous medium, respectively.

Because of the null volumetric liquid flux condition ($q = 0$), substituting Eq. (4) in Eq. (1a) yields the following differential relationship:

$$\gamma_w \frac{dh}{dx} = \frac{d\Pi}{dx} - \frac{d\bar{\Pi}}{dx} - \bar{c}_{sk}F\frac{d\bar{\varphi}}{dx} \tag{7}$$

Integration of Eq. (7) between the specimen boundaries results in the following physical identification of ω_g:

$$\omega_g = \left(1 - \frac{\Delta\bar{\Pi}}{\Delta\Pi}\right) - \bar{c}_{sk}F\frac{\Delta\bar{\varphi}}{\Delta\Pi} \tag{8}$$

where $\Delta\bar{\Pi}$ and $\Delta\bar{\varphi}$ are the differences in the osmotic pressure and in the electric potential of the pore solution across the porous medium, respectively.

Eq. (8) allows the different mechanisms that contribute to determining the measured reflection coefficient to be appreciated. The first contribution to ω_g, which is represented by the chemico-osmotic component $\left(\Omega_c = 1 - \frac{\Delta\bar{\Pi}}{\Delta\Pi}\right)$ and is only related to the ionic partition effect, tends to drive solvent from the dilute solution side to the concentrated solution side, provided that the electrochemical valences of the cation species do not differ. Under such an assumption, Ω_c ranges from zero for a porous medium without semipermeable properties to unity for a porous medium that behaves like a perfect anion exclusionary membrane. While the former asymptotic behaviour, i.e., $\Omega_c \simeq 0$ as $\bar{\psi} \to 0$, is self-evident, as the suppression of the ionic partition effect results in equality between $\Delta\bar{\Pi}$ and $\Delta\Pi$, proof of the latter asymptotic behaviour, i.e., $\Omega_c \simeq 1$ as $\bar{\psi} \to -\infty$, can be found by considering the definition of $\Delta\bar{\Pi}$:

$$\Delta\bar{\Pi} = RT\left(\sum_{cations}\Delta\bar{c}_i + \sum_{anions}\Delta\bar{c}_i\right) \tag{9}$$

where $\Delta\bar{c}_i$ is the difference in the pore solution concentration of the i-th ionic species across the porous medium.

If $\bar{c}_{sk}$ does not vary over the length of the porous medium, the following relationship can be derived from Eq. (3):

$$\sum_{cations} z_i\Delta\bar{c}_i + \sum_{anions} z_i\Delta\bar{c}_i = 0 \tag{10}$$

As the clay soil is hypothesised to behave as an ideal semipermeable membrane, the summations restricted to anions in both Eqs. (9) and (10) result to be equal to zero, so that $\Delta\bar{\Pi}$ is also observed to be annulled when the pore solution consists of cation species with the same electrochemical valences.

The second contribution to ω_g is represented by the electro-osmotic component $\left(\Omega_e = -\bar{c}_{sk}F\frac{\Delta\bar{\varphi}}{\Delta\Pi}\right)$ and is controlled by the so-called diffusion potential, $\Delta\bar{\varphi}$, which arises to enforce the condition of null electric current density when the mobilities of the ionic species differ from each other. Therefore, $\Delta\bar{\varphi}$ is obtained by substituting Eq. (1b) in Eq. (5) for $q = 0$ and integrating between the specimen boundaries:

$$\Delta \bar{\varphi} = -\frac{RT}{F} \int_{x_B}^{x_T} \sum_{i=1}^{N} \frac{z_i D_{0,i}}{\sum_{j=1}^{N} z_j^2 \bar{c}_j D_{0,j}} \frac{d\bar{c}_i}{dx} dx \tag{11}$$

where x_T and x_B are the coordinates of the top and bottom boundaries of the clay specimen along the macroscopic transport direction, respectively.

As discussed in detail by Yaroshchuk (1995), further study of Eq. (11) lets us to conclude that large deviations in the measured reflection coefficient from theoretical predictions based on pure chemico-osmosis, up to the limit cases of positive ($\omega_g \gg 1$) and negative ($\omega_g \ll 0$) anomalous osmosis, are not likely to be observed if only one cation species is present in the solution, regardless of the number of anion species that are produced by the electrolyte dissociation, as the magnitude of Ω_e is negligible. The presence of at least two cation species is necessary to cause such deviations and, when their electrochemical valences are the same, their aqueous-phase diffusion coefficients have to differ. In this latter situation, the contribution of diffusion induced electro-osmosis to the measured reflection coefficient may be comparable to or even greater than that associated with chemico-osmosis.

2.2. Calculation of the diffusion potential

Although an antiderivative of the integrand that appears in Eq. (11) is easily found for the case of single-electrolyte solutions (Dominijanni et al. 2019b), the calculation of the diffusion potential for electrolyte mixtures is not so straightforward. A general solution that holds for an arbitrary number of ionic species was presented by Helfferich (1962), but the assessment of the diffusion potential by means of this method is quite cumbersome and time consuming. Nevertheless, approximate analytical solutions can be obtained through the introduction of simplifying hypotheses, such as the one based on the so-called "constant-field assumption" (Goldman 1943) which has been widely adopted to study the electrical properties of biological tissues and synthetic membranes (e.g., Fatt and Ginsborg 1958; Chandler and Meves 1965; Walz et al. 1969; Gunn and Curran 1971; Sjodin 1980; Hahn and Woermann 1996). According to this latter approach, the Nernst-Planck equation is linearised with respect to the electric potential gradient, thus it is assumed that $\bar{\varphi}$ varies linearly over the length of the porous medium. Substituting the steady-state molar flux of the i-th ionic species, $(J_i)_{ss}$, which results from an integration of Eq. (1b) between the specimen boundaries, in Eq. (5) yields the following implicit solution for the diffusion potential:

$$\sum_{i=1}^{N} z_i^2 D_{0,i} \frac{\bar{c}_{i,T} \exp\left(\frac{z_i F}{RT} \Delta \bar{\varphi}\right) - \bar{c}_{i,B}}{\exp\left(\frac{z_i F}{RT} \Delta \bar{\varphi}\right) - 1} = 0 \tag{12}$$

where $\bar{c}_{i,T}$ and $\bar{c}_{i,B}$ are the concentrations of the i-th ionic species in the pore solution at the top and bottom boundaries of the clay specimen, respectively.

When the system consists of two 1:1-type electrolytes with a common anion (e.g., KCl and HCl), the implicit solution given by Eq. (12) reduces to the following explicit solution for the diffusion potential:

$$\Delta \bar{\varphi} = \frac{RT}{F} \cdot \ln\left(\frac{D_{0,1} \bar{c}_{1,B} + D_{0,2} \bar{c}_{2,B} + D_{0,3} \bar{c}_{3,T}}{D_{0,1} \bar{c}_{1,T} + D_{0,2} \bar{c}_{2,T} + D_{0,3} \bar{c}_{3,B}}\right) \tag{13}$$

where the subscripts 1, 2 and 3 refer to the two monovalent cation species and the single monovalent anion species, respectively.

Once $\Delta \bar{\varphi}$ has been calculated, $(J_i)_{ss}$ is obtained directly as follows:

$$(J_i)_{ss} = -\frac{n z_i D_i^* F}{RT} \frac{\Delta \bar{\varphi}}{L} \frac{\bar{c}_{i,T} \exp\left(\frac{z_i F}{RT} \Delta \bar{\varphi}\right) - \bar{c}_{i,B}}{\exp\left(\frac{z_i F}{RT} \Delta \bar{\varphi}\right) - 1} \tag{14}$$

and the concentration profile of the i-th ionic species in the pore solution, $\bar{c}_i(x)$, is given by:

$$\bar{c}_i(x) = \bar{c}_{i,B} \frac{1 - \exp\left(\frac{z_i F}{RT} \Delta \bar{\varphi} \frac{x_T - x}{L}\right)}{1 - \exp\left(\frac{z_i F}{RT} \Delta \bar{\varphi}\right)} + \bar{c}_{i,T}$$
$$\cdot \frac{1 - \exp\left(-\frac{z_i F}{RT} \Delta \bar{\varphi} \frac{x - x_B}{L}\right)}{1 - \exp\left(-\frac{z_i F}{RT} \Delta \bar{\varphi}\right)} \tag{15}$$

where $L = x_T - x_B$ is the length of the porous medium.

Even though the calculation approach based on the constant-field assumption accounts for the effect that is related to the nonlinearity in the ionic concentration profiles, an error is introduced by the hypothesis of linearity in the electric potential of the pore solution, thus leading to an approximate evaluation of $\Delta \bar{\varphi}$. As the conditions under which this hypothesis is acceptable cannot be determined in advance, an original closed-form analytical solution to the problem of calculating $\Delta \bar{\varphi}$, without any mathematical approximation, is illustrated hereafter. The following discussion is restricted to steady-state and null volumetric liquid flux conditions, in the presence of two monovalent cations and a single monovalent anion, but the solution can readily be extended to systems containing three ionic species with any electrochemical valences.

Combining the Nernst-Planck equations for the ionic molar fluxes, J_i (Eq. (1b)), at $q = 0$ with the conditions of electroneutrality in the pore solution (Eq. (3)) and null electric current density (Eq. (5)) allows the gradient in the electric potential of the membrane phase to be eliminated, as well as the flux and concentration of one of the two cations:

$$J_1 = -n\tau_m \left(D_1^1 \frac{d\bar{c}_1}{dx} + D_1^3 \frac{d\bar{c}_3}{dx}\right) \tag{16a}$$

$$J_3 = -n\tau_m \left(D_3^1 \frac{d\bar{c}_1}{dx} + D_3^3 \frac{d\bar{c}_3}{dx}\right) \tag{16b}$$

where

$$D_1^1 = D_{0,1}\left(1 + \bar{c}_1 \frac{D_{0,2} - D_{0,1}}{W}\right) \tag{17a}$$

$$D_1^3 = D_{0,1}\bar{c}_1 \frac{D_{0,3} - D_{0,2}}{W} \tag{17b}$$

$$D_3^1 = D_{0,3}\bar{c}_3 \frac{D_{0,1} - D_{0,2}}{W} \tag{17c}$$

$$D_3^3 = D_{0,3}\left(1 + \bar{c}_3 \frac{D_{0,2} - D_{0,3}}{W}\right) \tag{17d}$$

$$W = \bar{c}_1(D_{0,1} - D_{0,2}) + \bar{c}_3(D_{0,2} + D_{0,3}) + D_{0,2}\bar{c}_{sk} \tag{17e}$$

The $(J_3)_{ss}$ to $(J_1)_{ss}$ ratio at steady state is noticed to be invariant with respect to the position within the porous medium:

$$r = \frac{(J_3)_{ss}D_{0,1}}{(J_1)_{ss}D_{0,3}} \tag{18}$$

where the dimensionless r parameter does not depend on the x-coordinate.

Substituting Eqs. (16a) and (16b) in Eq. (18) and collecting terms yields the following differential relationship:

$$\frac{d\bar{c}_3}{d\bar{c}_1} = \frac{\alpha + \beta\bar{c}_3}{\gamma + \delta\bar{c}_1 + \varepsilon\bar{c}_3} \tag{19}$$

where

$$\alpha = rD_{0,2}\bar{c}_{sk} \tag{20a}$$

$$\beta = (D_{0,2} - D_{0,1}) + r(D_{0,2} + D_{0,3}) \tag{20b}$$

$$\gamma = D_{0,2}\bar{c}_{sk} \tag{20c}$$

$$\delta = (D_{0,1} - D_{0,2}) + r(D_{0,2} - D_{0,3}) \tag{20d}$$

$$\varepsilon = 2D_{0,2} \tag{20e}$$

When the terms α and γ are equal to zero, i.e., when the porous medium does not exhibit semipermeable properties, Eq. (19) reduces to the same one originally derived by Gose (1963) with a view to studying the diffusion of mixed electrolytes in the absence of ionic partition mechanisms. As such, the solution derived by Gose (1963) can be interpreted as a particular case of the more general solution proposed here, which is suitable to account for the electrical phenomena that are ascribed to the fixed negative charge of the solid skeleton.

Eq. (19) can be integrated between the boundaries of the clay layer through the method of the separation of variables:

$$\frac{\bar{c}_{3,T} - \eta}{\bar{c}_{3,B} - \eta} = \left[\frac{\varepsilon + (\delta - \beta)\frac{\bar{c}_{1,T} - \vartheta}{\bar{c}_{3,T} - \eta}}{\varepsilon + (\delta - \beta)\frac{\bar{c}_{1,B} - \vartheta}{\bar{c}_{3,B} - \eta}}\right]^{\frac{\beta}{\delta - \beta}} \tag{21}$$

where

$$\eta = -\frac{\alpha}{\beta} \tag{22a}$$

$$\vartheta = \frac{\alpha\varepsilon - \gamma\beta}{\beta\delta} \tag{22b}$$

The nonlinear equation given by Eq. (21), which generally admits multiple solutions, has to be solved for r by trial and error. As the solution of interest is the physically

acceptable one, a guess (approximate) r' value to start the iterative procedure can be obtained according to the constant-field assumption, thus substituting Eqs. (13) and (14) in Eq. (18):

$$r' = \frac{D_{0,1}(\bar{c}_{1,T}\bar{c}_{3,T} - \bar{c}_{1,B}\bar{c}_{3,B}) + D_{0,2}(\bar{c}_{2,T}\bar{c}_{3,T} - \bar{c}_{2,B}\bar{c}_{3,B})}{D_{0,2}(\bar{c}_{1,T}\bar{c}_{2,B} - \bar{c}_{1,B}\bar{c}_{2,T}) + D_{0,3}(\bar{c}_{1,T}\bar{c}_{3,T} - \bar{c}_{1,B}\bar{c}_{3,B})} \tag{23}$$

Once the r parameter has been determined for the given boundary conditions, the diffusion potential is obtained according to the following derivation. First, the Nernst-Planck equation is rewritten in a more concise form:

$$J_i = -n\tau_m D_{0,i} \exp\left(-z_i \frac{F}{RT}\bar{\varphi}\right)$$
$$\cdot \frac{d}{dx}\left[\bar{c}_i \exp\left(z_i \frac{F}{RT}\bar{\varphi}\right)\right] \tag{24}$$

The condition of null electric current density, if combined with the definition of r given by Eq. (18), allows $(J_1)_{ss}$ and $(J_2)_{ss}$ to be related to each other:

$$(J_2)_{ss} = (J_1)_{ss}\left(r\frac{D_{0,3}}{D_{0,1}} - 1\right) \tag{25}$$

Finally, substituting Eq. (24) in Eq. (25) yields the following differential relationship:

$$\frac{d\left[\bar{c}_2 \exp\left(\frac{F}{RT}\bar{\varphi}\right)\right]}{d\left[\bar{c}_1 \exp\left(\frac{F}{RT}\bar{\varphi}\right)\right]} = \frac{D_{0,1}}{D_{0,2}}\left(r\frac{D_{0,3}}{D_{0,1}} - 1\right) \tag{26}$$

which can be integrated between the boundaries of the clay layer to obtain an analytical expression for the diffusion potential:

$$\Delta\bar{\varphi} = \frac{RT}{F} \cdot \ln\left[\frac{D_{0,2}\bar{c}_{2,B} - D_{0,1}\left(r\frac{D_{0,3}}{D_{0,1}} - 1\right)\bar{c}_{1,B}}{D_{0,2}\bar{c}_{2,T} - D_{0,1}\left(r\frac{D_{0,3}}{D_{0,1}} - 1\right)\bar{c}_{1,T}}\right] \tag{27}$$

3. Interpretation of the Tang et al. (2014, 2015) experimental data

The results obtained by Tang et al. (2014, 2015) on a bentonite amended compacted clay have here been interpreted to provide insight into the fundamental mechanisms that are responsible for the coupling between the fluxes of water and charged solutes through fine-grained soils, focusing on the relative contribution of such mechanisms to the laboratory-scale determination of the reflection coefficient in both single and multi-electrolyte systems.

Tang et al. (2014) performed a multi-stage membrane test on a soil specimen that was obtained by mixing a locally available natural clay, known as Fukakusa clay, with 5% powdered sodium bentonite (by dry weight). After being compacted inside a rigid wall cell with a water content close to the optimum value of 23.2%, and then being saturated by immersion in deaerated deionised water (DW) and flushed to remove the soluble salts from the pore solution, the bentonite amended clay was tested by circu-

lating DW through the bottom porous stone, while sequentially injecting aqueous solutions with potassium chloride (KCl) concentrations of 0.5, 1, 5, 10 and 50 mM into the top porous stone under a null volumetric liquid flux condition. Achievement of the latter condition was guaranteed thanks to the use of a closed circulation loop, whereby the flow rates of the solution injected into and withdrawn from the top porous stone were imposed equal to each other.

The steady-state ω_g values, which are reported in Table 1 and plotted in Fig. 1 as a function of the source KCl concentration at the top specimen boundary, $c_{KCl,T}$, have been interpreted, via the theoretical model described in the previous section, for a value of the fixed charge concentration, $\bar{c}_{sk}$, equal to 5 mM. This value of $\bar{c}_{sk}$, which allows the observed decrease in the reflection coefficient with increasing KCl concentration to be accurately simulated apart from the isolated case of the ω_g value measured at $c_{KCl,T} = 1$ mM, is consistent with the one obtained by Dominijanni et al. (2018) for an unmixed pure sodium bentonite ($\bar{c}_{sk} \approx 30$ mM), given that the lower bentonite content of the specimen tested by Tang et al. (2014) is expected to result in a lower value of the fixed charge concentration. In the presence of a single electrolyte that dissociates into monovalent ionic species with similar diffusivities ($D_{0,K} = 1.96 \cdot 10^{-9}$ m²/s, $D_{0,Cl} = 2.03 \cdot 10^{-9}$ m²/s), the osmotic behaviour is shown to be dominated by chemico-osmosis, as the diffusion potential that is necessary to suppress the electric current density is negligible.

Tang et al. (2015) repeated the above multi-stage membrane test adding hydrochloric acid (HCl) to the aqueous solution circulating through the top porous stone in order to maintain a pH of 4, while leaving all the other testing conditions unchanged. The steady-state ω_g values, which are reported in Table 1, differ slightly from those determined by Tang et al. (2015), who did not account for the contribution of HCl in the calculation of the osmotic pressure difference across the clay specimen.
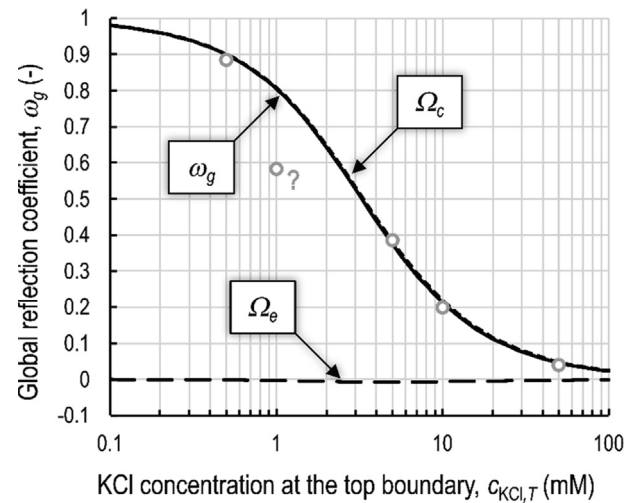

Fig. 1. Global reflection coefficient, ω_g, obtained from the multi-stage membrane test performed by Tang et al. (2014) under pH neutral conditions (pH = 7.0) at the top specimen boundary (open grey symbols), and the theoretical interpretation based on $\bar{c}_{sk} = 5$ mM (continuous line). The chemico-osmotic, Ω_c, and electro-osmotic, Ω_e, contributions to ω_g are highlighted with short-dashed and long-dashed lines, respectively.

As shown in Fig. 2, while the addition of HCl did not cause any appreciable variation in the osmotic behaviour for the highest source KCl concentration ($c_{KCl,T} = 50$ mM), a decrease in ω_g, i.e., with respect to the pH neutral conditions, occurred for the low-to-medium source KCl concentrations. Tang et al. (2015) explained such a detrimental effect on the membrane behaviour as being due to a partial dissolution of the bentonite crystalline structure under acidic conditions, which in turn resulted in larger void spaces and a reduced influence of the diffuse double layers. Although the aforementioned process cannot be excluded, calculations based on the evidence presented by Amram and Ganor (2005) have demonstrated that, even when a uniform pH profile equal to 4 is assumed across the specimen, the bentonite mass loss resulting from

Table 1
Results of the multi-stage membrane tests performed by Tang et al. (2014, 2015) on bentonite amended compacted clay.

pH at the top specimen boundary	$c_{KCl,T}$ (mM)	$c_{HCl,T}$ (mM)	$c_{KCl,B}$ (mM)	$c_{HCl,B}$ (mM)	$(\Delta h)_{ss}$ (m)	$\Delta\Pi$ (kPa)	ω_g (–)
7.0	0.5	0	0	0	0.218	2.42	0.885
	1	0	0	0	0.287	4.84	0.583
	5	0	0	0	0.950	24.18	0.385
	10	0	0	0	0.985	48.35	0.200
	50	0	0	0	1.003	241.77	0.041
4.0	1	0.1	0	0	0.297	5.40	0.539
	5	0.1	0	0	0.846	25.02	0.332
	10	0.1	0	0	0.863	49.54	0.171
	50	0.1	0	0	0.907	245.75	0.036

Note: $c_{KCl,T}$ and $c_{KCl,B}$, KCl concentrations of the solutions injected into the top and bottom porous stones, respectively; $c_{HCl,T}$ and $c_{HCl,B}$, HCl concentrations of the solutions injected into the top and bottom porous stones, respectively; $(\Delta h)_{ss}$, difference in the measured steady-state hydraulic head of the bulk solution across the specimen; $\Delta\Pi$, difference in the osmotic pressure of the bulk solution across the specimen; ω_g, global reflection coefficient.
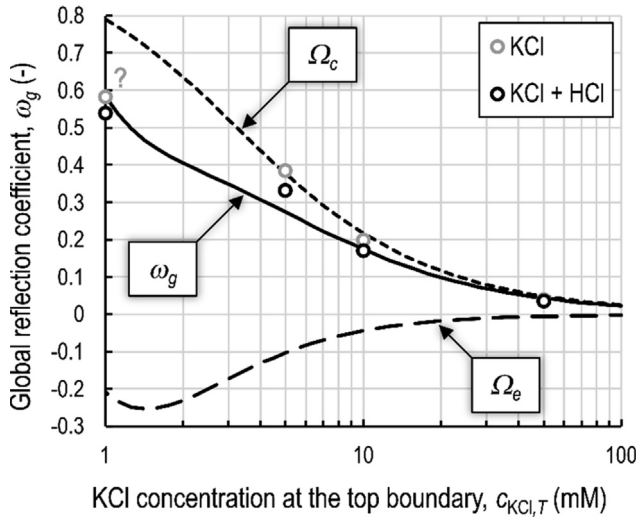
Fig. 2. Global reflection coefficient, ω_g, obtained from the multi-stage membrane test performed by Tang et al. (2015) under acidic conditions (pH = 4.0) at the top specimen boundary (open black symbols), and the theoretical interpretation based on $\bar{c}_{sk} = 5$ mM (continuous line). The chemico-osmotic, Ω_c, and electro-osmotic, Ω_e, contributions to ω_g are highlighted with short-dashed and long-dashed lines, respectively.

this pH is probably only about 0.1% relative to the initial mass of the bentonite, thus producing a negligible impact on the macroscopic semipermeable properties. This conclusion is consistent with that of Shackelford (1994), who reported on the basis of the literature that clay dissolution is not likely until the pH decreases to below a value of about 2.

A physically sound interpretation of the observed phenomenon, presented in Fig. 2, which allows the dependence of the reflection coefficient on $c_{KCl,T}$ to be simulated as accurately as in the case of single-salt testing solutions, has been achieved for the diffusion potential calculated through Eq. (27) and the same value of the fixed charge concentration calibrated with respect to the pH neutral conditions ($\bar{c}_{sk} = 5$ mM). Such an interpretation, which requires the use of the actual (measured) values of KCl and HCl concentrations at the bottom specimen boundary ($c_{KCl,B} = 4 \cdot 10^{-4}$ mM, $c_{HCl,B} = 6 \cdot 10^{-5}$ mM) to prevent unreliable predictions of the electro-osmotic effect from being obtained for the lowest source KCl concentration ($c_{KCl,T} = 1$ mM), suggests that diffusion induced electro-osmosis, which arises from the different mobilities of H^+ and K^+ ions in aqueous solution ($D_{0,H} = 9.31 \cdot 10^{-9}$ m^2/s), should be regarded as being responsible for the measured decrease in the reflection coefficient. The proposed interpretation thus explains, from a mechanistic viewpoint, the observed deviations in the osmotic behaviour from pure chemico-osmosis, without the need to postulate the existence of unproven contributions such as, for instance, the so-called "diffusion-osmosis" invoked by Olsen et al. (1990), who assumed that solutes diffusing in response to their concentration gradients are able to impose a net transfer of momentum to the water molecules.

As can also be noted from Fig. 2, while the case of pure chemico-osmosis is correlated with a single inflection point in the curve that depicts the dependence of the reflection coefficient on $c_{KCl,T}$, the build-up of diffusion induced electro-osmosis results in multiple inflection points. This latter peculiar behaviour can be ascribed to the initial increase in the relative contribution of electro-osmosis upon an increase in $c_{KCl,T}$, as can be expected considering the increase in the availability of K^+ ions at the top specimen boundary and, hence, the possibility for H^+ and K^+ ions to diffuse against each other when the behaviour of the porous medium approaches that of a perfect anion exclusionary membrane (Shackelford and Daniel 1991). However, a further increase in $c_{KCl,T}$ is detrimental to the semipermeable properties of the porous medium and, in a similar way to chemico-osmosis, causes a gradual decrease in the extent of electro-osmosis, which eventually vanishes when the ionic partition effect is suppressed. The superposition of the aforementioned pore-scale phenomena should therefore be regarded as being responsible for the bell-shaped curve of the electro-osmotic component.

The magnitude of the error of $\Delta\bar{\varphi}$ associated with the use of the approximate solution, given by Eq. (13), in lieu of the exact one, has been quantified and evidenced to be negligible for the testing conditions considered by Tang et al. (2015) when the source KCl concentration is sufficiently low, as shown in Figs. 3 and 4. However, the error has been noticed to increase upon an increase in the source KCl concentration of up to 38% at $c_{KCl,T} = 50$ mM, thus suggesting caution should be exercised in the use of the Goldman (1943) equation for the calculation of the diffusion potential across clay liners.

Finally, with the purpose of further elucidating the pore-scale phenomena underlying the build-up of diffusion
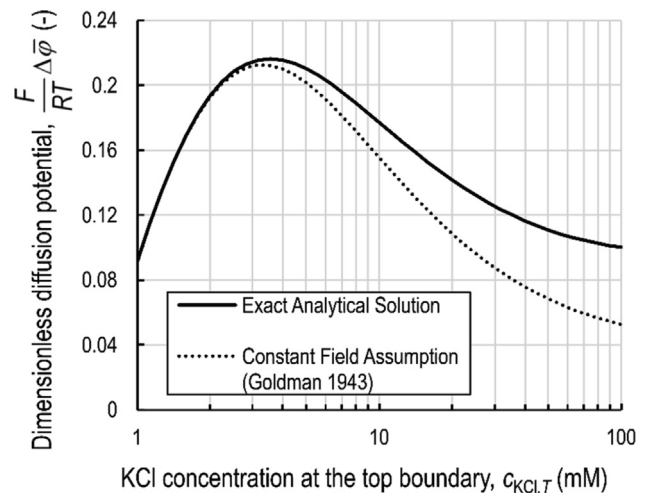

Fig. 3. Calculated diffusion potential, $\Delta\bar{\varphi}$, for the boundary electrolyte concentrations of the multi-stage membrane test performed by Tang et al. (2015) under acidic conditions (pH = 4.0): comparison between the exact analytical solution derived in this study and the approximate solution based on the constant-field assumption.
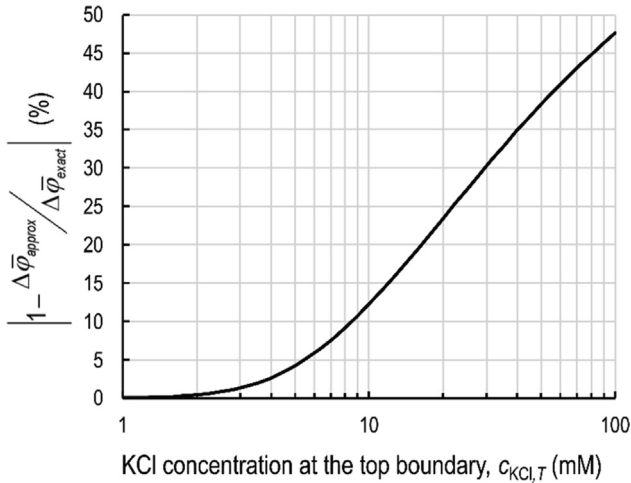
Fig. 4. Percent error in the diffusion potential calculated using the approximate solution, $\Delta\bar{\varphi}_{approx}$, relative to that calculated using the exact analytical solution, $\Delta\bar{\varphi}_{exact}$, for the boundary electrolyte concentrations of the multi-stage membrane test performed by Tang et al. (2015) under acidic conditions (pH = 4.0).

test performed by Tang et al. (2015), since the constant-field assumption is certainly acceptable at $c_{KCl,T} = 1$ mM and $c_{HCl,T} = 0.1$ mM. On the basis of the aforementioned concentration profiles, which are presented in Fig. 5, and the Nernst-Planck equation for electrically charged porous media, which is given by Eq. (1b), the addition of HCl to the solution circulating through the top specimen boundary is found to result in the upward diffusion of H^+ ions from the bottom to the top porous stone, i.e., in the opposite direction to that of K^+ ions, with the system approaching a condition of pure counter-diffusion due to the low permeability of the clay specimen to Cl^- ions. If any other driving force were not superimposed onto the ionic concentration gradients, a surplus of positive and negative electric charge would be accumulated at the top and bottom boundaries, respectively, as a result of purely diffusive transport. A positive diffusion potential, with the cathode corresponding to the bottom specimen boundary and the anode to the top specimen boundary, is thus generated to "speed up" the slower K^+ ions and "slow down" the faster H^+ ions, thereby preventing any charge unbalance from occurring. Such an electrically driven migration of cations towards the cathode is responsible for a net transfer of momentum to the water

induced electro-osmosis, the ionic concentration profiles in the pore solution have been calculated according to Eq. (15), with reference to the first stage of the membrane
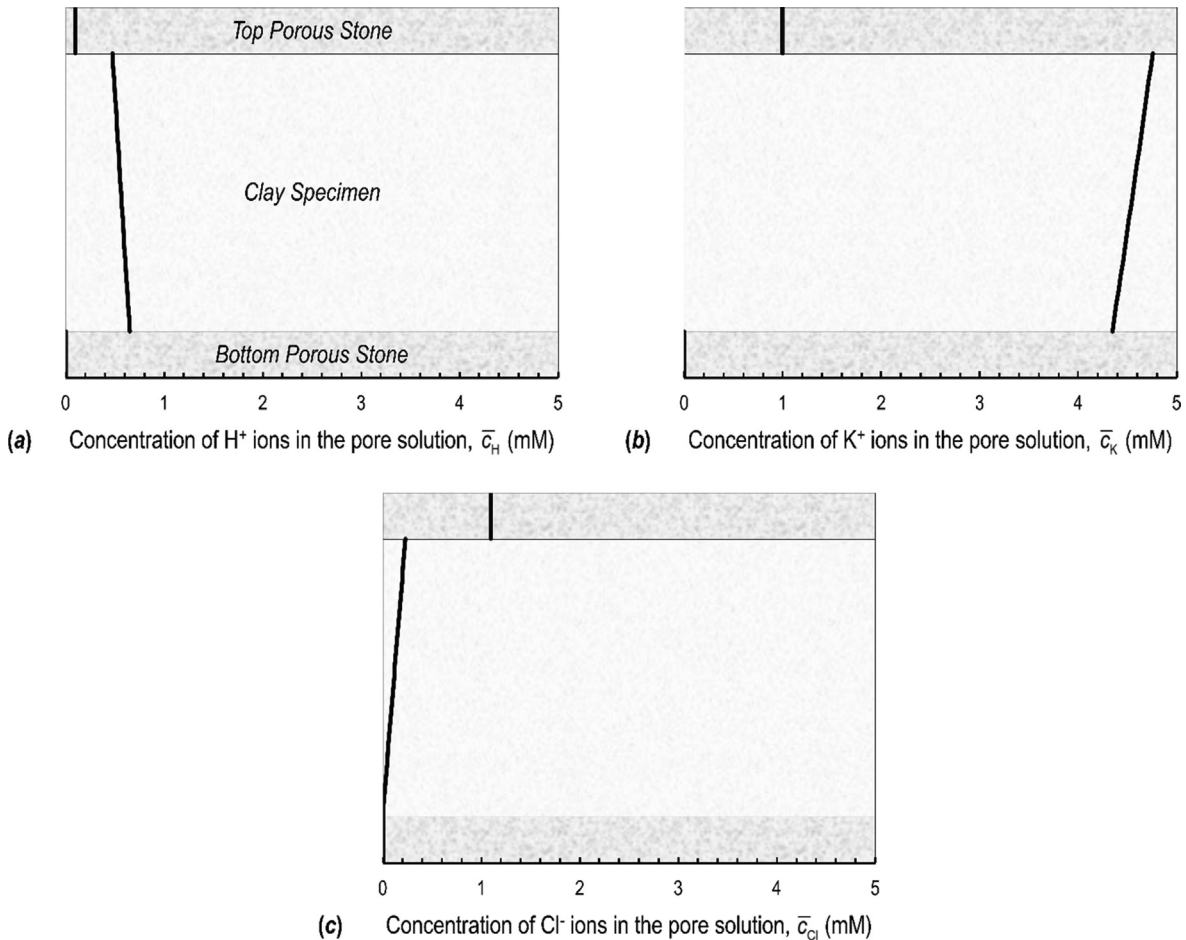

Fig. 5. Ionic concentration profiles in the pore solution calculated for the first stage of the membrane test performed by Tang et al. (2015) at $c_{KCl,T} = 1$ mM and $c_{HCl,T} = 0.1$ mM: (a) hydrogen (H^+) ions; (b) potassium (K^+) ions; (c) chloride (Cl^-) ions.

molecules in the direction of the more negative potential and, on account of the $q = 0$ condition, for the build-up of an electro-osmotic contribution to the measured hydraulic head difference, $(\Delta h)_{ss}$.

4. Conclusions

On the basis of a physically sound theoretical framework, which allows the macroscopic effect of the electrical interactions that occur at the pore scale to be modelled, the non-hydraulic component of the volumetric liquid flux through active clays, as driven by a gradient in the ionic concentrations, has been shown to be dominated by chemico-osmosis whenever the permeant solution contains a single electrolyte. However, the same mechanistic model has also suggested that large deviations from pure chemico-osmosis may be observed in aqueous solutions of mixed electrolytes, due to the increasing influence of an electro-osmotic effect that is caused by the different diffusivities of the cations dissolved in the pore solution.

An exact analytical solution to the problem of calculating the diffusion potential, which in turn controls the magnitude of the aforementioned electro-osmotic effect, has been derived to allow the osmotic phenomena in three-ionic systems to be quantitatively analysed, in this way overcoming the limitations entailed by the constant-field assumption. The relative importance of chemico-osmosis and diffusion induced electro-osmosis has been investigated through the theoretical interpretation of the experimental results of Tang et al. (2014, 2015), which refer to a bentonite amended compacted clay permeated with aqueous mixtures of KCl and HCl.

Further research, aimed at studying the significance of diffusion induced electro-osmosis in engineered clay barriers used for chemical containment purposes, is recommended. Besides the need for an experimental investigation on the conditions under which anomalous values of the reflection coefficient (i.e., ω_g values outside the 0 to 1 range) are predicted, the possibility of modelling transient-state conditions through an extension of the proposed theoretical framework should be explored, with the aim of assessing whether cation exchange phenomena are correlated with the build-up of an appreciable electro-osmotic effect, even when clay specimens are tested in contact with single-salt aqueous solutions. Finally, the rationality of the hypothesis of a null volumetric liquid flux through the clay layer, although appropriate for the theoretical interpretation of the ω_g values resulting from membrane testing under closed-system conditions, needs to be critically evaluated for the case of open-system conditions. The latter conditions, which may be representative of actual field scenarios, are associated with the development of a streaming potential, whose magnitude, relative to the diffusion potential, should be quantified accordingly.

Declaration of Competing Interest

The authors declare that they have no known competing financial interests or personal relationships that could have appeared to influence the work reported in this paper.

References

Abrams, I., Sollner, K., 1943. The structure of the collodion membrane and its electrical behavior: VI. The protamine-collodion membrane, a new electropositive membrane. J. Gen. Physiol. 26 (4), 369–379. https://doi.org/10.1085/jgp.26.4.369.

Amram, K., Ganor, J., 2005. The combined effect of pH and temperature on smectite dissolution rate under acidic conditions. Geochim. Cosmochim. Acta 69 (10), 2535–2546. https://doi.org/10.1016/j.gca.2004.10.001.

Appelo, C.A.J., Wersin, P., 2007. Multicomponent diffusion modeling in clay systems with application to the diffusion of tritium, iodide, and sodium in Opalinus Clay. Environ. Sci. Technol. 41 (14), 5002–5007. https://doi.org/10.1021/es0629256.

Bohnhoff, G.L., Shackelford, C.D., 2013. Improving membrane performance via bentonite polymer nanocomposite. Appl. Clay Sci. 86, 83–98. https://doi.org/10.1016/j.clay.2013.09.017.

Bohnhoff, G.L., Shackelford, C.D., 2015. Salt diffusion through a bentonite-polymer composite. Clays Clay Miner. 63 (3), 145–162. https://doi.org/10.1346/CCMN.2015.0630301.

Chandler, W.K., Meves, H., 1965. Voltage clamp experiments on internally perfused giant axons. J. Physiol. 180 (4), 788–820. https://doi.org/10.1113/jphysiol.1965.sp007732.

Cwirko, E.H., Carbonell, R.G., 1989. Transport of electrolytes in charged pores: Analysis using the method of spatial averaging. J. Colloid Interface Sci. 129 (2), 513–531. https://doi.org/10.1016/0021-9797(89)90466-9.

Di Emidio, G., Mazzieri, F., Verastegui-Flores, R.D., Van Impe, W., Bezuijen, A., 2015. Polymer-treated bentonite clay for chemical-resistant geosynthetic clay liners. Geosynth. Int. 22 (1), 125–137. https://doi.org/10.1680/gein.14.00036.

Dominijanni, A., Manassero, M., 2005. Modelling osmosis and solute transport through clay membrane barriers. In: Proceedings of the Geo-Frontiers Congress, Austin, Texas, USA, 24-26 January 2005. *Edited by* A. Alshawabkleh, C.H. Benson, P.J. Culligan, J.C. Evans, B.A. Gross, D. Narejo, K.R. Reddy, C.D. Shackelford, and J.G. Zornberg. American Society of Civil Engineers, Reston, Virginia, USA, pp. 349-360. https://doi.org/10.1061/40789(168)19.

Dominijanni, A., Manassero, M., 2012a. Modelling the swelling and osmotic properties of clay soils. Part I: The phenomenological approach. Int. J. Eng. Sci. 51, 32–50. https://doi.org/10.1016/j.ijengsci.2011.11.003.

Dominijanni, A., Manassero, M., 2012b. Modelling the swelling and osmotic properties of clay soils. Part II: The physical approach. Int. J. Eng. Sci. 51, 51–73. https://doi.org/10.1016/j.ijengsci.2011.11.001.

Dominijanni, A., Manassero, M., Vanni, D., 2006. Micro/macro modeling of electrolyte transport through semipermeable bentonite layers. *In* Proceedings of the 5th International Congress on Environmental Geotechnics, Cardiff, Wales, UK, 26-30 June 2006. *Edited by* H.R. Thomas. Thomas Telford, London, England, UK, Vol. 2, pp. 1123–1130.

Dominijanni, A., Manassero, M., Puma, S., 2013. Coupled chemical-hydraulic-mechanical behaviour of bentonites. Géotechnique 63 (3), 191–205. https://doi.org/10.1680/geot.SIP13.P.010.

Dominijanni, A., Guarena, N., Manassero, M., 2018. Laboratory assessment of semipermeable properties of a natural sodium bentonite. Can. Geotech. J. 55 (11), 1611–1631. https://doi.org/10.1139/cgj-2017-0599.

Dominijanni, A., Fratalocchi, E., Guarena, N., Manassero, M., Mazzieri, F., 2019a. Critical issues in the determination of the bentonite cation

exchange capacity. Géotechnique Letters 9 (3), 205–210. https://doi.org/10.1680/jgele.18.00229.

Dominijanni, A., Guarena, N., Manassero, M., 2019b. Phenomenological analysis and physical interpretation of the reflection coefficient of clays. In: Proceedings of the 8th International Congress on Environmental Geotechnics, Hangzhou, China, 28 October - 1 November 2018. *Edited by* L. Zhan, Y. Chen, and A. Bouazza. Springer, Singapore, Vol. 3, pp. 156-163. https://doi.org/10.1007/978-981-13-2227-3_19.

Elrick, D.E., Smiles, D.E., Baumgartner, N., Groenevelt, P.H., 1976. Coupling phenomena in saturated homo-ionic montmorillonite: I. Experimental. Soil Sci. Soc. Am. J. 40 (4), 490–491. https://doi.org/10.2136/sssaj1976.03615995004000040014x.

Evans, J.C., Shackelford, C.D., Yeo, S.S., Henning, J.T., 2008. Membrane behavior of soil-bentonite slurry-trench cutoff walls. Soil Sediment Contam. 17 (4), 316–322. https://doi.org/10.1080/15320380802143880.

Eykholt, G.R., Daniel, D.E., 1994. Impact of system chemistry on electroosmosis in contaminated soil. J. Geotech. Geoenviron. Eng. 120 (5), 797–815. https://doi.org/10.1061/(ASCE)0733-9410(1994)120:5(797).

Fatt, P., Ginsborg, B.L., 1958. The ionic requirements for the production of action potentials in crustacean muscle fibres. J. Physiol. 142 (3), 516–543. https://doi.org/10.1113/jphysiol.1958.sp006034.

Fritz, S.J., 1986. Ideality of clay membranes in osmotic processes: A review. Clays Clay Miner. 34 (2), 214–223. https://doi.org/10.1346/CCMN.1986.0340212.

Fritz, C.J., Scalia, J., Shackelford, C.D., Malusis, M.A., 2020. Determining maximum chemico-osmotic pressure difference across clay membranes. J. Geotech. Geoenviron. Eng. 146 (1), 06019018. https://doi.org/10.1061/(ASCE)GT.1943-5606.0002196.

Fu, X.L., Zhang, R., Reddy, K.R., Li, Y.C., Yang, Y.L., Du, Y.J., 2021a. Membrane behavior and diffusion properties of sand/SHMP-amended bentonite vertical cutoff wall backfill exposed to lead contamination. Eng. Geol. 284. https://doi.org/10.1016/j.enggeo.2021.106037 106037.

Fu, X.L., Wu, H.L., Zhang, R., Jiang, Z.Y., Reddy, K.R., Du, Y.J., 2021b. Heavy metals containment by vertical cutoff walls backfilled with novel reactive magnesium-activated slag-bentonite-sand: Membrane and diffusion behavior. J. Cleaner Prod. 328. https://doi.org/10.1016/j.jclepro.2021.129623 129623.

Fujita, H., Kobatake, Y., 1968. Interpretation of anomalous osmosis. J. Colloid Interface Sci. 27 (4), 609–615. https://doi.org/10.1016/0021-9797(68)90092-1.

Goldman, D.E., 1943. Potential, impedance, and rectification in membranes. J. Gen. Physiol. 27 (1), 37–60. https://doi.org/10.1085/jgp.27.1.37.

Gose, E.E., 1963. Diffusion of three ionic species in liquid solution. J. Chem. Phys. 39 (3), 735–738. https://doi.org/10.1063/1.1734317.

Groenevelt, P.H., Bolt, G.H., 1969. Non-equilibrium thermodynamics of the soil-water system. J. Hydrol. 7 (4), 358–388. https://doi.org/10.1016/0022-1694(69)90092-4.

Groenevelt, P.H., Elrick, D.E., 1976. Coupling phenomena in saturated homoionic montmorillonite: II. Theoretical. Soil Sci. Soc. Am. J. 40 (6), 820–823. https://doi.org/10.2136/sssaj1976.03615995004000060011x.

Gross, R.J., Osterle, J.F., 1968. Membrane transport characteristics of ultrafine capillaries. J. Chem. Phys. 49 (1), 228–234. https://doi.org/10.1063/1.1669814.

Guarena, N., Dominijanni, A., Manassero, M., 2020. From the design of bottom landfill liner systems to the impact assessment of contaminants on underlying aquifers. Innov. Infrastruct. Solut. 5 (1), 2. https://doi.org/10.1007/s41062-019-0251-y.

Guarena, N., Dominijanni, A., Manassero, M., 2021a. Relative contribution of chemico-osmosis and electro-osmosis to the experimental determination of the reflection coefficient in semipermeable clay soils. JGS Special Publication 9 (4), 111–117. https://doi.org/10.3208/jgssp.v09.cpeg012.

Guarena, N., Dominijanni, A., Manassero, M., 2021b. Relevance of chemico-osmotic and electro-osmotic phenomena in bentonite-based barriers. In: Barla, M., Di Donna, A., Sterpi, D. (Eds.), . In: Lecture Notes in Civil Engineering, Vol. 126. Springer, Cham, Switzerland, pp. 903–910. https://doi.org/10.1007/978-3-030-64518-2_107.

Gunn, R.B., Curran, P.F., 1971. Membrane potentials and ion permeability in a cation exchange membrane. Biophys. J . 11 (7), 559–571. https://doi.org/10.1016/S0006-3495(71)86235-5.

Hahn, O., Woermann, D., 1996. Osmotic properties of a phenolsulfonic acid formaldehyde cation exchange membrane in contact with mixed aqueous electrolyte solutions. J. Membr. Sci. 117 (1–2), 197–206. https://doi.org/10.1016/0376-7388(96)00053-1.

Helfferich, F., 1962. Ion exchange. McGraw-Hill, New York, USA.

Henning, J.T., Evans, J.C., Shackelford, C.D., 2006. Membrane behavior of two backfills from field-constructed soil-bentonite cutoff walls. J. Geotech. Geoenviron. Eng. 132 (10), 1243–1249. https://doi.org/10.1061/(ASCE)1090-0241(2006)132:10(1243).

Hijnen, H.J.M., Smit, J.A.M., 1995. The effect of the pH on electrolyte transport through microporous membranes bearing either weakly or strongly dissociating acid groups. A theoretical analysis using the space-charge model for a cylindrical capillary. J. Membr. Sci. 99 (3), 285–302. https://doi.org/10.1016/0376-7388(94)00264-Y.

Hijnen, H.J.M., Van Daalen, J.V., Smit, J.A.M., 1985. The application of the space-charge model to the permeability properties of charged microporous membranes. J. Colloid Interface Sci. 107 (2), 525–539. https://doi.org/10.1016/0021-9797(85)90205-X.

Jacazio, G., Probstein, R.F., Sonin, A.A., Yung, D., 1972. Electrokinetic salt rejection in hyperfiltration through porous materials. Theory and experiment. J. Phys. Chem. 76 (26), 4015–4023. https://doi.org/10.1021/j100670a023.

Jougnot, D., Revil, A., Leroy, P., 2009. Diffusion of ionic tracers in the Callovo-Oxfordian clay-rock using the Donnan equilibrium model and the formation factor. Geochim. Cosmochim. Acta 73 (10), 2712–2726. https://doi.org/10.1016/j.gca.2009.01.035.

Kang, J.B., Shackelford, C.D., 2010. Membrane behavior of compacted clay liners. J. Geotech. Geoenviron. Eng. 136 (10), 1368–1382. https://doi.org/10.1061/(ASCE)GT.1943-5606.0000358.

Kang, J.B., Shackelford, C.D., 2011. Consolidation enhanced membrane behavior of a geosynthetic clay liner. Geotext. Geomembr. 29 (6), 544–556. https://doi.org/10.1016/j.geotexmem.2011.07.002.

Keijzer, T.J.S., Kleingeld, P.J., Loch, J.P.G., 1999. Chemical osmosis in compacted clayey material and the prediction of water transport. Eng. Geol. 53 (2), 151–159. https://doi.org/10.1016/S0013-7952(99)00028-9.

Kemper, W.D., Quirk, J.P., 1972. Ion mobilities and electric charge of external clay surfaces inferred from potential differences and osmotic flow. Soil Sci. Soc. Am. J. 36 (3), 426–433. https://doi.org/10.2136/sssaj1972.03615995003600030019x.

Kemper, W.D., Rollins, J.B., 1966. Osmotic efficiency coefficients across compacted clays. Soil Sci. Soc. Am. J. 30 (5), 529–534. https://doi.org/10.2136/sssaj1966.03615995003000050005x.

Kemper, W.D., Shainberg, I., Quirk, J.P., 1972. Swelling pressures, electric potentials, and ion concentrations: Their role in hydraulic and osmotic flow through clays. Soil Sci. Soc. Am. J. 36 (2), 229–236. https://doi.org/10.2136/sssaj1972.03615995003600020012x.

Lakshminarayanaiah, N., 1965. Transport phenomena in artificial membranes. Chem. Rev. 65 (5), 491–565. https://doi.org/10.1021/cr60237a001.

Leroy, P., Revil, A., Coelho, D., 2006. Diffusion of ionic species in bentonite. J. Colloid Interface Sci. 296 (1), 248–255. https://doi.org/10.1016/j.jcis.2005.08.034.

Malusis, M.A., Daniyarov, A.S., 2016. Membrane efficiency and diffusive tortuosity of a dense prehydrated geosynthetic clay liner. Geotext. Geomembr. 44 (5), 719–730. https://doi.org/10.1016/j.geotexmem.2016.05.006.

Malusis, M.A., Shackelford, C.D., 2002a. Chemico-osmotic efficiency of a geosynthetic clay liner. J. Geotech. Geoenviron. Eng. 128 (2), 97–106. https://doi.org/10.1061/(ASCE)1090-0241(2002)128:2(97).

Malusis, M.A., Shackelford, C.D., 2002b. Coupling effects during steady-state solute diffusion through a semipermeable clay membrane.

Environ. Sci. Technol. 36 (6), 1312–1319. https://doi.org/10.1021/es011130q.

Malusis, M.A., Shackelford, C.D., Maneval, J.E., 2012. Critical review of coupled flux formulations for clay membranes based on nonequilibrium thermodynamics. J. Contam. Hydrol. 138–139, 40–59. https://doi.org/10.1016/j.jconhyd.2012.06.003.

Malusis, M.A., Kang, J.B., Shackelford, C.D., 2015. Restricted salt diffusion in a geosynthetic clay liner. Environ. Geotech. 2 (2), 68–77. https://doi.org/10.1680/envgeo.13.00080.

Malusis, M.A., Scalia, J., Norris, A.S., Shackelford, C.D., 2020. Effect of chemico-osmosis on solute transport in clay barriers. Environ. Geotech. 7 (7), 447–456. https://doi.org/10.1680/jenge.17.00109.

Malusis, M., Dominijanni, A., Scalia, J., Guarena, N., Sample-Lord, K., Bohnhoff, G., Shackelford, C., Manassero, M., 2021. Assessing the influence of chemico-osmosis on solute transport in bentonite membranes based on combined phenomenological and physical modeling. JGS Special Publication 9 (2), 37–44. https://doi.org/10.3208/jgssp.v09.cpeg023.

Manassero, M., 2020. Second ISSMGE R. Kerry Rowe Lecture: On the intrinsic, state, and fabric parameters of active clays for contaminant control. Can. Geotech. J. 57 (3), 311–336. https://doi.org/10.1139/cgj-2019-0033.

Manassero, M., Dominijanni, A., 2003. Modelling the osmosis effect on solute migration through porous media. Géotechnique 53 (5), 481–492. https://doi.org/10.1680/geot.2003.53.5.481.

Manassero, M., Dominijanni, A., Guarena, N., 2018. Modelling hydro-chemo-mechanical behaviour of active clays through the fabric boundary surface. In: Wu, W., Yu, H.S. (Eds.), In Proceedings of the China Europe Conference on Geotechnical Engineering. Springer Series in Geomechanics and Geoengineering, Cham, Switzerland, Vol. 2, Cham, Switzerland, pp. 1618–1626. https://doi.org/10.1007/978-3-319-97115-5_157.

Mazzieri, F., Di Emidio, G., Van Impe, P.O., 2010. Diffusion of calcium chloride in a modified bentonite: Impact on osmotic efficiency and hydraulic conductivity. Clays Clay Miner. 58 (3), 351–363. https://doi.org/10.1346/CCMN.2010.0580306.

Medved, I., Černý, R., 2013. Osmosis in porous media: A review of recent studies. Microporous Mesoporous Mater. 170, 299–317. https://doi.org/10.1016/j.micromeso.2012.12.009.

Meier, A.J., Shackelford, C.D., 2017. Membrane behavior of compacted sand-bentonite mixture. Can. Geotech. J. 54 (9), 1284–1299. https://doi.org/10.1139/cgj-2016-0708.

Mitchell, J.K., 1991. Conduction phenomena: From theory to geotechnical practice. Géotechnique 41 (3), 299–340. https://doi.org/10.1680/geot.1991.41.3.299.

Mitchell, J.K., Soga, K., 2005. Fundamentals of soil behavior, 3rd ed. John Wiley & Sons, New York, USA.

Mitchell, J.K., Greenberg, J.A., Witherspoon, P.A., 1973. Chemico-osmotic effects in fine-grained soils. J. Soil Mech. Found. Div. 99 (SM4), 307–322.

Musso, G., Cosentini, R.M., Dominijanni, A., Guarena, N., Manassero, M., 2017. Laboratory characterization of the chemo-hydro-mechanical behaviour of chemically sensitive clays. Rivista Italiana di Geotecnica 51 (3), 22–47. https://doi.org/10.19199/2017.3.0557-1405.022.

Olsen, H.W., Yearsley, E.N., Nelson, K.R., 1989. Chemical causes of groundwater movement. In: Groundwater Contamination. Edited by L.M. Abriola. Publication 185, IAHS, pp. 65-72.

Olsen, H.W., Yearsley, E.N., Nelson, K.R., 1990. Chemico-osmosis versus diffusion-osmosis. Transportation Research Record 1288, Transportation Research Board, Washington, D.C., pp. 15–22.

Revil, A., Linde, N., 2006. Chemico-electromechanical coupling in microporous media. J. Colloid Interface Sci. 302 (2), 682–694. https://doi.org/10.1016/j.jcis.2006.06.051.

Röttger, H., Woermann, D., 1993. Osmotic properties of polyelectrolyte membranes: Positive and negative osmosis. Langmuir 9 (5), 1370–1377. https://doi.org/10.1021/la00029a034.

Sample-Lord, K.M., Shackelford, C.D., 2018. Membrane behavior of unsaturated sodium bentonite. J. Geotech. Geoenviron. Eng. 144 (1), 04017102. https://doi.org/10.1061/(ASCE)GT.1943-5606.0001803.

Sasidhar, V., Ruckenstein, E., 1982. Anomalous effects during electrolyte osmosis across charged porous membranes. J. Colloid Interface Sci. 85 (2), 332–362. https://doi.org/10.1016/0021-9797(82)90003-0.

Schlögl, R., 1955. Zur theorie der anomalen osmose. Z. Phys. Chem. 3, 73–102. https://doi.org/10.1524/zpch.1955.3.1_2.073.

Schmid, G., 1950. Zur elektrochemie feinporiger kapillarsysteme I. Übersicht. Zeitschrift für Elektrochemie und angewandte physikalische. Chemie 54 (6), 424–430. https://doi.org/10.1002/bbpc.19500540610.

Shackelford, C.D., 1994. Waste-soil interactions that alter hydraulic conductivity. In: Proceedings of the Symposium Hydraulic Conductivity and Waste Contaminant Transport in Soil, San Antonio, Texas, 21-22 January 1993. Edited by D.E. Daniel, and S.J. Trautwein. STP 1142, ASTM, Philadelphia, Pennsylvania, USA, pp. 111–168. https://doi.org/10.1520/STP23887S.

Shackelford, C.D. 2013. Membrane behavior in engineered bentonite-based containment barriers: State of the art. In: Proceedings of the International Symposium on Coupled Phenomena in Environmental Geotechnics, Torino, Italy, 1-3 July 2013. Edited by M. Manassero, A. Dominijanni, S. Foti, and G. Musso. CRC Press/Balkema, Taylor & Francis Group, London, England, UK, pp. 45–60. https://doi.org/10.1201/b15004-7.

Shackelford, C.D., Daniel, D.E., 1991. Diffusion in saturated soil: I. Background. J. Geotech. Eng. 117 (3), 467–484. https://doi.org/10.1061/(ASCE)0733-9410(1991)117:3(467).

Shackelford, C.D., Meier, A.J., Sample-Lord, K.M., 2016. Limiting membrane and diffusion behavior of a geosynthetic clay liner. Geotext. Geomembr. 44 (5), 707–718. https://doi.org/10.1016/j.geotexmem.2016.05.009.

Shackelford, C.D., Lu, N., Malusis, M.A., Sample-Lord, K.M., 2019. Research challenges involving coupled flows in geotechnical engineering. In Geotechnical Fundamentals for Addressing New World Challenges. Springer Series in Geomechanics and Geoengineering, Cham, Switzerland, pp. 237–274. https://doi.org/10.1007/978-3-030-06249-1_9.

Sjodin, R.A., 1980. Contribution of Na/Ca transport to the resting membrane potential. J. Gen. Physiol. 76 (1), 99–108. https://doi.org/10.1085/jgp.76.1.99.

Smit, J.A.M., 1989. Reverse osmosis in charged membranes: Analytical predictions from the space-charge model. J. Colloid Interface Sci. 132 (2), 413–424. https://doi.org/10.1016/0021-9797(89)90256-7.

Tang, Q., Katsumi, T., Inui, T., Li, Z., 2014. Membrane behavior of bentonite-amended compacted clay. Soils Found. 54 (3), 329–344. https://doi.org/10.1016/j.sandf.2014.04.019.

Tang, Q., Katsumi, T., Inui, T., Li, Z., 2015. Influence of pH on the membrane behavior of bentonite amended Fukakusa clay. Sep. Purif. Technol. 141, 132–142. https://doi.org/10.1016/j.seppur.2014.11.035.

Tasaka, M., Kondo, Y., Nagasawa, M., 1969. Anomalous osmosis through charged membranes. J. Phys. Chem. 73 (10), 3181–3188. https://doi.org/10.1021/j100844a002.

Van Impe, P.O., Van Impe, W.F., Mazzieri, F., Constales, D., 2003. Coupled flow model for three-ion advective-dispersive-reactive transport in consolidating clay liners. In: Proceedings of the 13th European Conference on Soil Mechanics and Geotechnical Engineering, Prague, Czech Republic, 25-28 August 2003. Balkema, Rotterdam, Netherlands, Vol. 3, pp. 227–232.

van't Hoff, J.H. 1887. The role of osmotic pressure in the analogy between solutions and gases. Zeitschrift für physikalische Chemie, 1, 481–508.

Walz, D., Bamberg, E., Läuger, P., 1969. Nonlinear electrical effects in lipid bilayer membranes: I. Ion injection. Biophys. J. 9 (9), 1150–1159. https://doi.org/10.1016/S0006-3495(69)86442-8.

Woermann, D., 1968. Transport of ions against their concentration gradient across cation-exchange membranes with very small mechanical permeabilities. J. Am. Chem. Soc. 90 (12), 3020–3025. https://doi.org/10.1021/ja01014a005.

Yaroshchuk, A.E., 1995. Osmosis and reverse osmosis in fine-charged diaphragms and membranes. Adv. Colloid Interface Sci. 60 (1–2), 1–93. https://doi.org/10.1016/0001-8686(95)00246-M.

Yaroshchuk, A.E., 2011. Transport properties of long straight nano-channels in electrolyte solutions: A systematic approach. Adv. Colloid Interface Sci. 168 (1–2), 278–291. https://doi.org/10.1016/j.cis.2011.03.009.

Yeo, S.S., Shackelford, C.D., Evans, J.C., 2005. Membrane behavior of model soil-bentonite backfills. J. Geotech. Geoenviron. Eng. 131 (4), 418–429. https://doi.org/10.1061/(ASCE)1090-0241(2005)131:4(418).

Yeung, A.T., Mitchell, J.K., 1993. Coupled fluid, electrical and chemical flows in soil. Géotechnique 43 (1), 121–134. https://doi.org/10.1680/geot.1993.43.1.121.